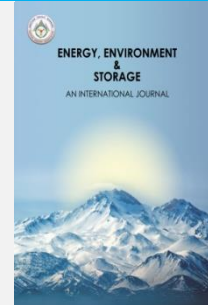


Energy, Environment and Storage

Journal Homepage: www.enenstrg.com



Detailed Experimental Investigation of A Spark Ignition Engine in A Wide Range of Work

Melih YILDIZ¹, Bilge ALBAYRAK ÇEPER¹

¹ Erciyes University, Dept. of Aerospace Engineering, Kayseri, balbayrak@erciyes.edu.tr

¹ Iğdır University, Department of Mechanical Engineering, Iğdır, melih.yildiz@igdir.edu.tr

ABSTRACT. For years, the goal of vehicle manufacturers; combustion control of spark ignition engines, ease of passage between the various cycles For years, the goal of vehicle manufacturers; combustion control of spark ignition engines, ease of passage between the various cycles, low emission values of diesel engines, high fuel economy and output power, thereby achieving optimum values in internal combustion engines. In this context, to improve the engine performance and increase the volumetric and thermal efficiency of the engine in all operating conditions to minimize the power losses and to reduce the exhaust emissions in order to obtain the maximum power, most economical and without environmental pollution, continues to be updated. In this study, the optimum working map of the engine was obtained by considering the power, torque, specific fuel consumption, cylinder pressure, exhaust gas temperature, thermal efficiency, average effective pressure, heat dissipation rate and emissions of four stroke, two cylinder, spark ignition SI engine fuel.

Keywords: Spark ignition engine, Specific fuel consumption, BMEP, Emissions

Article History: Received: 12.10.2020; Revised: 25.04.2021; Accepted: 24.04.2021 Available online: 28.04.2021

Doi: <https://doi.org/10.52924/BBNP1133>

1. INTRODUCTION

Internal combustion engines use approximately one-third of the daily total world oil production. With the increase in the number of internal combustion engine vehicles, air pollution is rapidly increasing in parallel with the emissions they emit into the atmosphere. Researches on the efficient use of fuel in engines and reduction of pollutant emissions in exhaust gases continue at a great pace [1].

Internal combustion engines are classified as spark ignition (SI) and compression ignition (CI) engines according to their combustion characteristics. A conventional SI combustion can be characterized by flame formation and the development and spread of this flame. The initiation of the combustion reaction is achieved by controlling the spark plug ignition timing. In compression ignition engines, it starts with the spraying of fuel on the compressed air and self-ignition and continues. In both of these combustion events, the improvement of performance and exhaust emissions depends on an efficient combustion in a very short time. Adjusting a large number of parameters according to the operating conditions of the engine in order to keep the

combustion efficiency at the maximum level in all operating conditions of the engine will provide the most efficient conversion of fuel to energy. For this purpose, some operating parameters such as ignition advance, valve opening and closing times, compression ratio and air-fuel ratio are changed depending on engine speed and load [2]. In addition, the researchers investigated different alternative fuel additions to gasoline and investigated their effects on engine performance and emissions.

opgöl et al. [3] examined the effects of these changes on exhaust emissions by changing the air excess coefficient, ignition advance, compression ratio and engine inlet air temperature in a single cylinder, four stroke, spark ignition engine. As a result of the experimental work carried out; They found that the increase in the ignition advance causes the reduction of CO emissions, and the increase in the ignition advance up to 30° KMA increases the HC emissions.

İsmail and Mehta [4] investigated the effects of adding hydrogen into gasoline on engine performance using mathematical modeling method in their study. The results they found in their study at different speeds and compression ratios found that

*Corresponding author: balbayrak@erciyes.edu.tr

hydrogen gas added to gasoline at different rates had a positive effect on engine performance.

Aktaş and Doğan [5] examined the effects of adding LPG to diesel fuel at different rates on engine performance and emissions in a single cylinder, compression ignition, four-stroke engine. In the study, the diesel engine was operated at the speed at which the maximum torque was obtained, and diesel fuel was used as a pilot fuel and LPG was added into the cylinder in different proportions by weight. They observed that with the addition of LPG to diesel fuel, NO_x and soot emissions improved and HC emissions increased. In addition, they found a decrease in fuel consumption and an increase in engine power with the addition of LPG at different rates in diesel engines.

In the studies of Özer and Vural [6], the possibility of acetylene gas as an alternative fuel in a spark ignition engine in terms of exhaust emissions was experimentally investigated. During the test, an internal combustion gasoline, single cylinder, four-stroke engine with a compression ratio of 8/1 and a maximum engine speed of 3600 rpm was used. If it is an experiment; the effect of adding 20% and 30% acetylene gas into the cylinder by increasing 400 rpm between 1600 rpm and 3200 rpm on the exhaust emissions was investigated. As a result of the investigations, it was observed that the addition of 20% and 30% acetylene gas worsened combustion. In addition, different rates of reductions in exhaust gas temperature, HC, CO, CO₂ and NO_x emissions were detected.

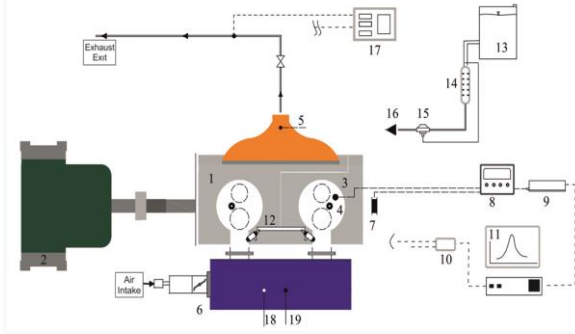
In this study, in order to contribute to the literature, the effects of different parameters on engine performance and emissions in a spark ignition engine were examined experimentally and the points where the combustion performance parameters were efficient in SI mode were revealed.

2. MATERIALS AND METHOD

Experimental studies were carried out on a four-stroke spark ignition Lombardini LGW520 engine in the Engines Laboratory of the Mechanical Engineering Department of Erciyes University. The technical features of the test engine are given in Table 1. The schematic view of the experimental setup is given in Figure 1.

Table 1: Test engine specifications.

Numbers of cylinders	2
Cylinder Volume	505 cc
Bore x Stroke	72x62 mm
Compression Ratio	10.7:1
Maximum Power	15 kW
Maximum Torque	34 Nm 2150rpm
Cooling type	Water cooled



- 1) Test engine, (2) Dynamometer, (3) Pressure sensor, (4) Spark plug, (5) Exhaust temperature thermocouple, (6) Throttle, (7) Encoder, (8) Amplifier, (9) Oscilloscope, (10) Data logger, (11) Computer, (12) Port type injector system, (13) Fuel tank, (14) Scale container, (15) Regulator, (16) Fuel pump, (17) Gas emission device, (18) Thermocouple, (19) Pressure sensor

Figure 1: Schematic experimental setup.

In the experimental study, a 50 kW hydraulic dynamometer was used to enable the internal combustion engine to operate and control under different load and speed conditions. With this dynamometer, different speed and torque values can be obtained by controlling the motor load with the water brake. Emission measurements were carried out using Bosch BAE-070 gas analyzer, whose technical specifications are given in Table 2. Emission measurements were taken at specific time intervals, for each operating point, 10 measurements were taken and the average of these values and measurement values were determined.

Table 2: Gas analyzer specifications

Parameter	Measuring range	Unit	Accuracy
HC	0-20,000	ppm	1.0
CO ₂	0-20	%	0.1
CO	0-15	%	0.001
O ₂	0-21.7	%	0.01
Lambda	0.6-1.2	-	0.001
NO _x	0-5,000	ppm	1.0

In-cylinder pressure measurements for pressure-based combustion analysis were performed with a Kistler 6053CC brand pressure sensor. This pressure sensor (Table 3) is realized with a connection point opening into the combustion chamber. In order to amplify the signals obtained during engine start-up, the Kistler5018A brand signal amplifier, whose technical specifications are given in Table 4, has been passed. It is set to a suitable mode and a low filtering range of 100 Hz in order to prevent irregularities in the form of slipping of signals due to noise, vibration and thermal shocks. In addition, the calibration values specified by the manufacturer were used to ensure that the signals obtained from the pressure sensor were correctly converted from voltage values to pressure units [bar]. In order to display and record these voltage values obtained

from the amplifier, Pico branded oscilloscope was used and recorded in PicoScope-Automotive software.

For determination of crankshaft angle position, rotary type encoder is used. This encoder, together with the intersection of the upper dead point (TDC) with the marked point on the encoder connection shaft, generates 3-4 V voltage at each 360o rotation and provides TDC signals. In this context, in order to adjust the encoder to the ÜÖN position, since the maximum pressure values obtained during the cycle without combustion will occur in the TDC, the pressure signals obtained from the cylinder to which the pressure sensor is connected have been used. During the experimental studies, the engine water temperature was kept at 85 ± 2 oC. Exhaust gas temperature measurement was carried out in the area close to the oxygen probe, 10 cm from the exhaust manifold outlet.

Table 3: Pressure sensor (Kistler6053CC) specifications

Measuring range	bar	0-250 bar
Calibration intervals	bar	0-50, 0-100, 0-150, 0-250
Accuracy	pC/bar	≈ -20
Natural frequency	kHz	160
Working range temperature	°C	-20 - 350

Table 4: Signal Amplifier specifications (Kistler 5018A).

Measuring Range	pC	$\pm 2 - 2.2 \times 10^5$
Measurement Errors		
<10 pC	%	< ± 2
<100 pC	%	< ± 0.6
≥ 100 pC	%	< ± 3
In signal drift mode	pC/s	< ± 0.03

3 RESULTS

The experiments were started with the studies carried out under full load at different speeds. Experimental studies were repeated for 80%, 50% and 30% load conditions, taking into account the torque values obtained under full load condition. In addition, experiments at different speeds were repeated, taking into account the effective pressure (BMEP) values with the brake medium (Figure 2).

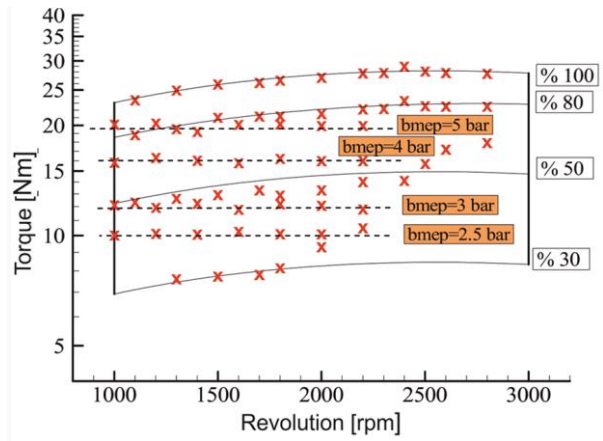


Figure 2: Experimental study points.

Torque, power and specific fuel consumption obtained at full load are given in Figure 3. As seen in Figure 3, the maximum torque value was obtained at 2300 rpm around 28 Nm under full load. Torque variation tends to decrease after this speed value. Specific fuel consumption, on the other hand, is high as expected at low speeds. With the increase of engine speed, specific fuel consumption decreases. This is due to the change in experimental modification. In other words, the specific fuel consumption decreases as the amount of increase in power is greater than the amount of fuel increasing per unit time.

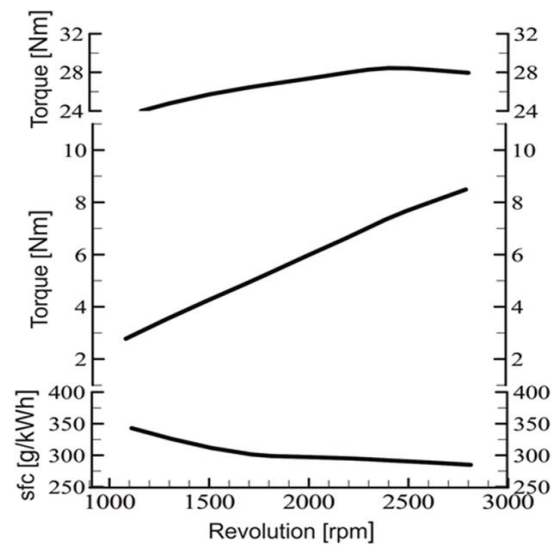


Figure 3: Engine performance characteristics (full load).

Figure 4 shows the ÖYT variation obtained according to different rotational speed and brake averaged effective pressure values. Specific fuel consumption values decrease with increasing BMEP value as shown in the figure and change between 297 g / kWh and 504 g / kWh. BMEP value expresses the average pressure obtained in the cylinder during the engine cycle and provides information about the load condition in the engine operating condition. Therefore, as the increase in engine load will increase engine power, the amount of fuel per unit power, in other words specific fuel consumption, has decreased.

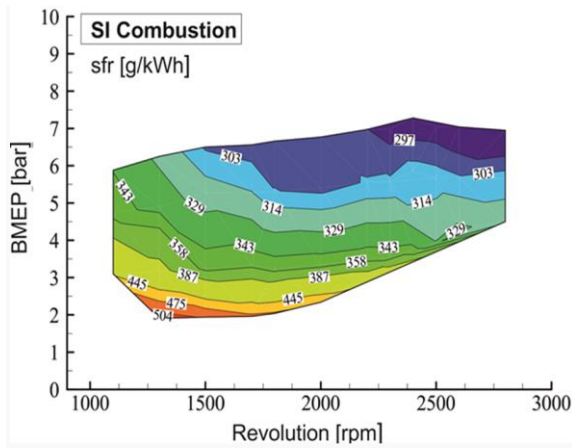


Figure 4: Specific fuel consumption [g / kWh] changes.

Figure 5 shows the distribution of brake thermal efficiency values obtained at different rotation speeds. As seen in the figure, the thermal efficiency change characteristic is similar to the ÖYT change. While brake thermal efficiency values reached maximum efficiency values in rotation speed and BMEP values, on the contrary, minimum values were obtained at low BMEP and speed values. The brake thermal efficiency values obtained varied between 0.17 and 0.29 in these operating ranges.

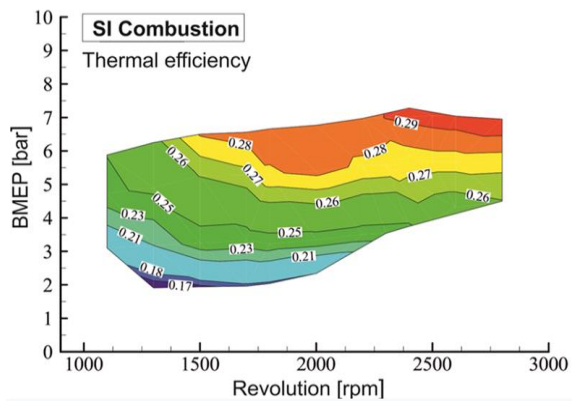


Figure 5: Brake thermal efficiency values.

The key emissions addressed in a spark ignition (SI) internal combustion engine are NO_x, HC and CO emission values. NO_x formation generally occurs due to three main factors. The first is the thermal NO_x formation that occurs in the high temperature zones formed inside the cylinder. Another formation mechanism is the formation of NO_x caused by the rapid reactions that occur especially in the rich parts of the cylinder. Finally, NO_x emission formations are caused by the N₂ molecules contained in the fuel. However, among these formation mechanisms, especially thermal NO_x emission formations are more effective [7]. Therefore, during the experimental studies, the exhaust gas outlet temperatures were measured and parametric evaluation was provided on NO_x formation. Figure 6 gives the distribution of exhaust gas temperature values measured at different loads and speeds. As can be seen in the figure, the exhaust gas outlet temperature increased with the increase of both the speed value and the BMEP value. On the other hand,

as seen in Figure 7, when the NO_x formations are evaluated by associating them with the exhaust outlet temperatures, it is observed that there is an increase in NO_x emissions, basically due to the increase in the exhaust gas outlet temperature (hence the increase in the average temperature inside the cylinder). However, as can be seen from the horizontal contour curves, it is understood that the change characteristic in NO_x formation changes especially as a function of the BMEP value. In addition, it is the change of these variation curves in the vertical curve ranges between 2300 rpm and 2400 rpm where the maximum torque occurs, in other words, depending on the rotation speed.

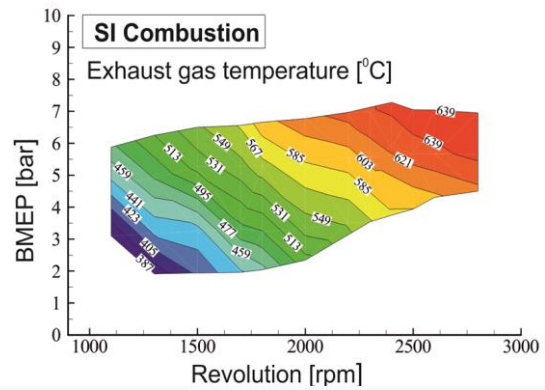


Figure 6. Exhaust gas temperature

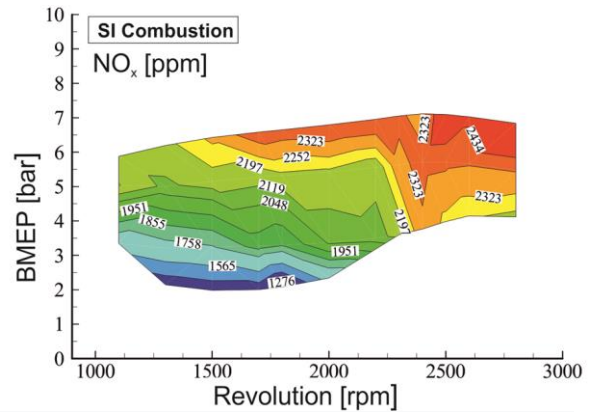


Figure 7. NO_x emissions.

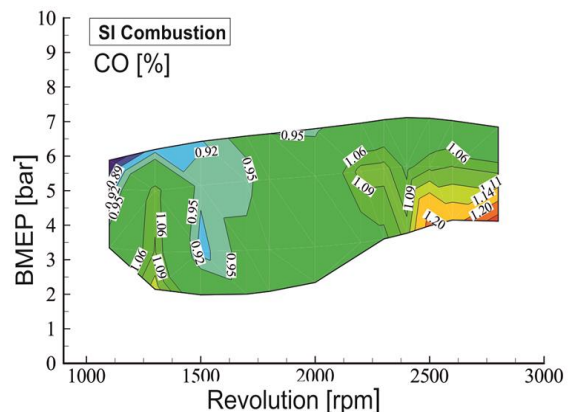


Figure 8. CO emissions.

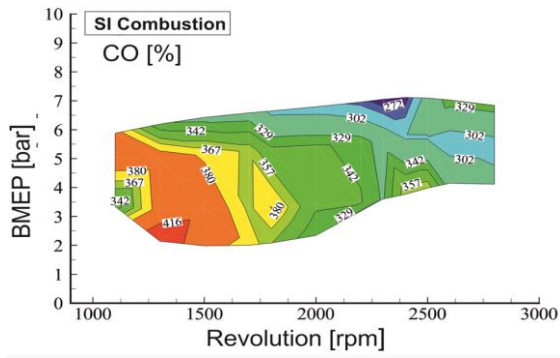


Figure 9. HC emissions.

While the temperature in the cylinder is also an important factor in the formation of CO emissions, the fuel-air mixture ratio, the homogeneity of the mixture in the cylinder, the dissociation reactions that occur due to high temperature are important factors. In the cylinder, especially in the cold regions close to the cylinder walls, it increases the CO emissions by reducing the oxidation of CO in CO₂ due to low temperature. On the other hand, it contributes to the formation of CO as there will not be the required O₂ amount for the reaction, due to the rich mixture of air-fuel ratio and / or the local rich mixture regions formed in the cylinder [8]. Figure 8 shows the distribution of CO emission values. While CO emissions were obtained in minimum concentration, especially around low speed and high BMEP values, they reached maximum values at medium load values at 2500 rpm. In general, it has been observed that there is no significant change in CO emission according to both speed and load conditions.

HC emission formation is again a function of in-cylinder temperature values, and local very poor or rich mixture regions affect the formation of HC. While local very rich mixing zones contribute to HC formation by preventing oxidation of the fuel due to low O₂ concentration, in very poor local regions, they prevent the combustion of the fuel by causing the flame to extinguish and provide HC formation. Along with these, the burning of thin film layers formed on the walls of the combustion chamber of the lubricating oil causes an increase in HC emissions [9]. Figure 9 shows the distribution of HC emission values measured at different BMEP and engine rotational speeds.

Figure 10 shows the pressure curves of 300 consecutive cycles and the pressure gradient of the mean cycle obtained with these pressure curves. This average cycle curve obtained represents the pressure change at the specified operating point of the internal combustion engine.

Figure 11 shows the pressure curves and pressure increase rates obtained at different rotation speeds and loads. As can be seen in the figure, a significant decrease has been observed in the in-cylinder

pressure values with the decrease in the load ratio. However, pressure increase rates also decrease with the decrease in the load ratio. The basic parameters obtained from these pressure curves are summarized in Table 5.

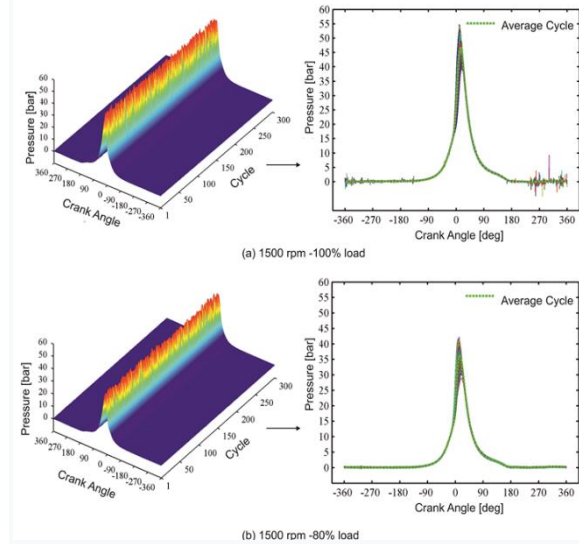


Figure 10. In-cylinder pressure curves.

Figure 12 shows the variation of the total heat dissipation with the crankshaft angle and the net heat dissipation rates. Heat release rate (HRR) gives information about the rate at which the combustion reaction occurs in an internal combustion engine [10]. As can be seen in Figure 12, the heat dissipation rate decreases significantly with the decrease in the load ratio, this is because the fuel-air filling in the cylinder decreases with the decrease in the load ratio. This situation is clearly seen from the change in the total amount of heat dissipation. On the other hand, the increase in the rotational speed increased the speed of the total heat dissipation amount.

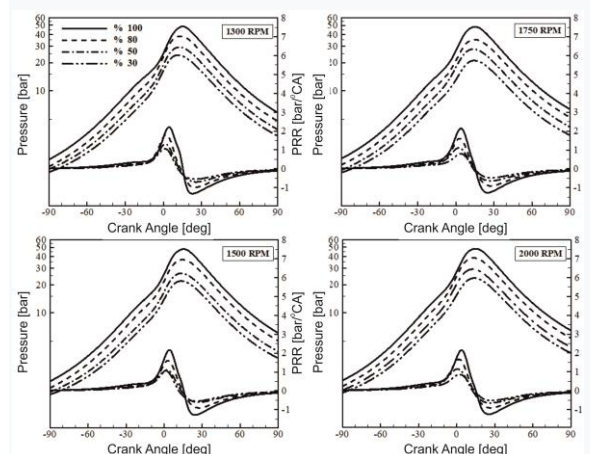


Figure 11. Variation of the pressure curves and pressure increase rates

Table 5. Pressure curves summarizes

1300 rpm				
Load rate	%100	%80	%50	%30
Pmaks. [bar]	48.70	38.11	29.14	24.10
Pmak_location [KMA]	15.30	13.40	12.50	11.50
(PRR)mak [bar/oKMA]	2.36	1.88	1.43	1.17
1500 rpm				
Pmaks. [bar]	47.90	36.87	26.37	21.92
Pmak_location [KMA]	10.90	11.80	15.40	17.20
(PRR)mak [bar/oKMA]	2.31	1.71	1.20	0.97
1750 rpm				
Pmaks. [bar]	48.15	35.26	27.84	21.06
Pmak_location [KMA]	15.30	14.60	13.80	14.50
(PRR)mak [bar/oKMA]	2.32	1.55	1.21	0.87
2000 rpm				
Pmaks. [bar]	47.20	33.20	26.78	21.58
Pmak_location [KMA]	15.70	14.80	13.60	14.60
(PRR)mak [bar/oKMA]	2.21	1.38	1.12	0.87

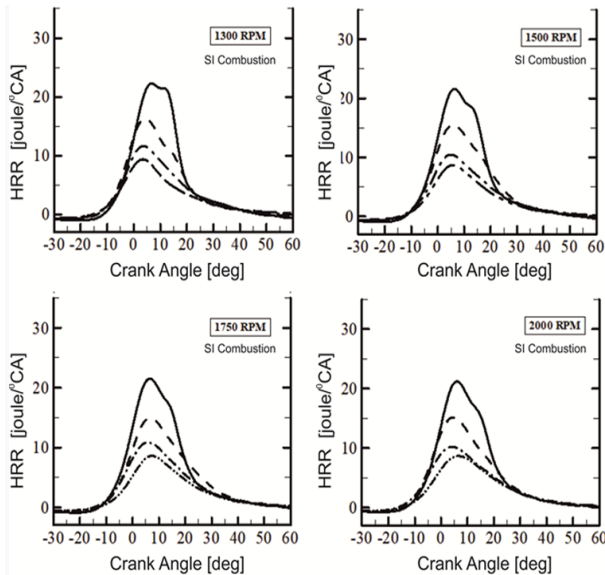


Figure 12: The change of total heat dissipation rates.

Another parameter obtained by combustion analysis is obtaining the burnt fuel ratio curve according to KMA [11]. Combustion start, combustion end and combustion durations can be determined by obtaining this curve.

In general, the Wiebe function and the Rassweiler & Withrow method are used to obtain the burnt fuel amount curve [11]. Wiebe function is a method used especially in numerical studies. In experimental studies, the Rassweiler & Withrow method is a more commonly used method. The Wiebe function can be arranged by adjusting the necessary coefficients with the curves obtained from Rassweiler & Withrow [12-14]. In Figure 13, the change curves of the burnt fuel ratios obtained by the Rassweiler & Withrow method are given at different load and speed values.

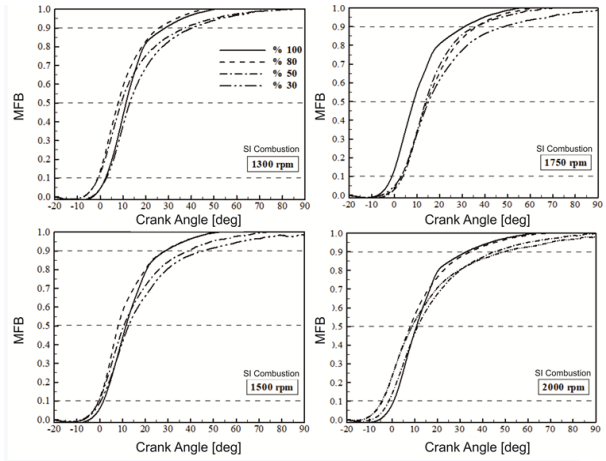


Figure 13. Burnt fuel ratio change curves

CA10, CA50 and CA90 points, which are important points in the burnt fuel ratio curve, are the KMA points corresponding to the value of 0.1, 0.5 and 0.9 of the burnt fuel ratio, respectively [15]. In theory, the burning time between CA10 and CA90 is considered. CA10 is also considered as the point where high-temperature combustion reactions begin and turbulent flame propagation begins with the development of the flame core in a spark-fueled engine. In a compression ignition engine, it is generally considered as CA5 and this value is evaluated as the ignition delay time [15]. The CA50 point takes place at this point of the maximum heat dissipation rate or at the KMA near this point [16]. Therefore, examining these points in combustion analysis gives important insights about the combustion time and combustion development [17]. Accordingly, the pressure development in the cylinder can be correlated.

In internal combustion engines, evaluation of cyclic variation can be considered as an indicator of stabilization in engine operation [18-22]. Figure 14 shows the values of the indicated mean effective pressure at different velocities and BMEP values.

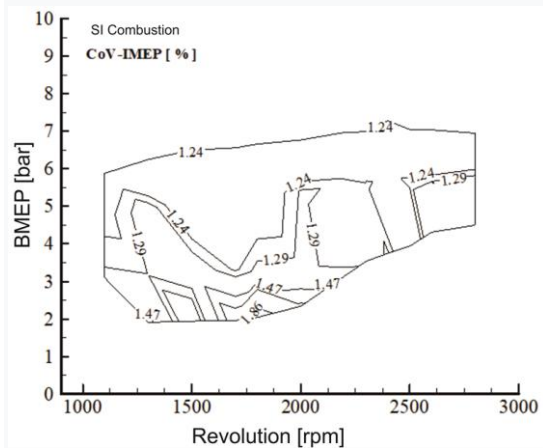


Figure 14: Indicated mean effective pressure coefficient of variation (CoVimep) variations

Considering the COVimep values, no significant change was observed with the speed and load status in SI combustion mode. The maximum value was obtained at low BMEP values of 1.86%. Since this coefficient of variation is too high, it will mean that

the cycle-to-cycle power generation of the motor is highly variable, so it will affect the motor operation stabilization. This value is generally limited to 5% in the literature [23]. Another coefficient of variation is the maximum pressure values inside the cylinder. This value is especially important in terms of combustion stabilization when it shows the variability of the maximum pressure values reached with heat dissipation. Figure 15 shows the variation of the maximum pressure variation coefficients in different motor rotational speed and BMEP values.

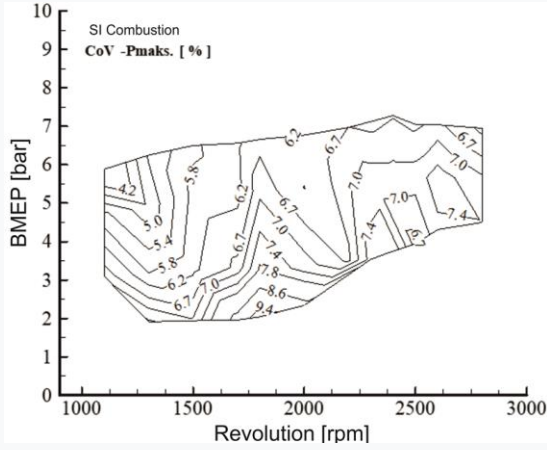


Figure 15: Change of maximum pressure coefficients of variation (CoVPmax)

Considering the COVPmax distributions, it is seen that the BMEP values rather than the rotation increase velocity affect the maximum pressure variation coefficient values. Especially in low velocity and high BMEP values, it is seen that the coefficient of variation is lower.

Acknowledgments

This study was completed with the support of TÜBİTAK 113M101 project and the authors are grateful to TÜBİTAK and Erciyes University.

REFERENCES

[1] Çırak B., Gürbüz H., Yapay sinir ağları kullanarak dizel motorlarda termal bariyer kaplamasının emisyonlara etkilerinin incelenmesi, Nevşehir Üniversitesi Fen Bilimleri Enstitüsü Dergisi 1, 24-35, 2012.

[2] Sekmen Y., Erduranlı P., Gölcü M., Salman M.S., Buji ile ateşlemeli motorlarda sıkıştırma oranı değişiminin performans parametrelerine etkisi, Pamukkale Üniversitesi Mühendislik Bilimleri Dergisi, 11(1), 23-30, 2005.

[3] Topgül T., Yücesu H.S., Okur M., Buji ile Ateşlemeli Bir Motorda Çalışma Parametrelerinin Egzoz Emisyonlarına Etkilerinin Deneysel Olarak İncelenmesi, Politeknik Dergisi, 8(1),43-47, 2005.

[4] Saleel I., Mehta P. S., Second Law Analysis of Hydrogen Air Combustion in a Spark Ignition Engine, International journal of hydrogen energy, 36 (1): 931-946, 2011.

[5] Aktaş A., Doğan O., Çift Yakıtlı Bir Dizel Motorda LPG Yüzdesinin Performans ve

Emisyonlara etkisi, Gazi Üniversitesi Mühendislik Mimarlık Fakültesi Dergisi, 25 (1):171- 178, 2010.

[6] Vural E., Özer S., Buji ateşlemeli motorlarda yakıtta asetilen gazı ilavesinin egzoz emisyonlarına etkisinin deneysel analizi, BEU Fen Bilimleri Dergisi 3(1), 24-34, 2014.

[7] Albayrak Ç. B., Yıldız M, Akansu S.O, Kahraman N. Performance and emission characteristics of an IC engine under SI, SI-CAI and CAI combustion modes, ENERGY, Vol. 136, p. 72-79, 2017.

[8] Canakcı M. An experimental study for the effects of boost pressure on the performance and exhaust emissions of a DI-HCCI gasoline engine. Fuel 2008(87):1503-14.

[9] Heywood, J.B. 1988. Internal Combustion Engine Fundamentals, McGraw-Hill, New York

[10] Yıldız, M., Akansu, S.O, Çeper, B.A. Computational study of EGR and excess air ratio effects on a methane fueled CAI engine. International Journal of Automotive Engineering and Technologies. 2015, (4);3:152-161.

[11] Stone R. Introduction to Internal Combustion Engines, Third Edition. Society of Automotive Engineers Inc. Warrendale, 1999.

[12] Yıldız, M., Albayrak Çeper, B. Zero-dimensional single zone engine modeling study on methane-fueled SI engine using single and double Wiebe functions, 9 th Sustainable Energy and Environmental Protection, Kayseri, Türkiye, 22-25 Eylül 2016, pp.208-215

[13] Yeliana, Y., Cooney, C., Worm, J., Michalek, D.J, Naber, J.D. Estimation of double-Wiebe function parameters using least square method for burn durations of ethanol-gasoline blends in spark ignition engine over variable compression ratios and EGR levels. Applied Thermal Engineering, 31(2011): 2213- 2220.

[14] Mittal M, Schock H. Fast mass-fraction-burned calculation using the net pressure method for real-time applications. Proceeding of the Institution of Mechanical Engineers, Part D: Journal of Automobile Engineering, 2008(223):389-394.

[15] Hunicz, J.,Kordos, P. An experimental study of fuelinjection strategies in CAI engine, Experimental Thermal and Fluid Science, 35(2011):243-252.

[16] Zhao H. Motivationdefinitionandhistory of HCCI/CAI engines. In: Zhao H, editor. HCCI and CAI Enginesforthe Automotive Industry, Woodhead Publishing Limited, 2007.

[17] Maurya, R.K, Agarwal, A.K. Experimental investigation on effect of intake air temperature and air-fuel ratio on cycle-to-cycle variations of HCCI combustion and performance, Applied Energy, 2011(88)1153-63.

[18] Kım, D.S, Kım M.Y, Lee, C.H. Combustion and emission characteristics of partial homogeneous charge compression ignition engine. Combust. Sci. and Tech. 177(2005):107-125

[19] Lee,C.H.,Lee K.H. An experimental study of the combustion characteristics in SCCI and CAI based on direct injection gasoline engine.

Experimental Thermal and Fluid Science, 31(2007):1121-32.

[20] Chen, T., Xie, H., Li, L., Zhang, L., Wang, X., Zhao, H. Methods to achieve HCCI/CAI combustion in 4VVAS gasoline engine, Applied Energy. 116(2014)41-51.

[21] Li, H. L., Neil, W. S., Chippor, W. Cycle-to-cycle variation of a HCCI engine operated with n-heptane. Spring Technical Meeting

Combustion Institute/Canadian Section, Paper 5;1-6, 2007

[22] Choi, S., Park, W., Lee, S., Min, K., Choi, H. Methods for in-cylinder EGR stratification and its effects on combustion and emission characteristics in a diesel engine, Energy, 36(2011):6948-59.

[23] Osborne, R. J., Li, G., Sapsford S. M., Stokes, J., Lake, T. H. Evaluation of HCCI for future Powertrains. SAE paper, 2003-01-0750